J Mater Sci: Mater Med (2008) 19:2669–2677
DOI 10.1007/s10856-008-3395-4

Synthesis and characterization of tricalcium phosphate with Zn and Mg based dopants

Weichang Xue · Kelli Dahlquist · Ashis Banerjee · Amit Bandyopadhyay · Susmita Bose

Received: 28 November 2007 / Accepted: 22 January 2008 / Published online: 13 February 2008

Abstract The purpose of this study is to prepare tricalcium phosphate (TCP) ceramic by dual dopants of magnesium (Mg) and zinc (Zn), and investigate the influence of dopants on the physical, mechanical and biological properties of TCP. TCP were synthesized with 1 wt% Mg, 0.3 wt% Zn and dual dopants using the precipitation process. Phase composition and microstructures were characterized. Mechanical properties and dissolution behavior in vitro were investigated. Human osteoblast cell culture was used to determine the influence of dopants on cell-materials interactions. XRD analysis indicated that Mg delayed phase transformation from β to α-TCP and pure β-TCP phase was obtained for Mg-doped TCP after sintered at 1250°C. Addition of Mg improved densification behavior of TCP. Compression strength also increased from 24.0 MPa to 77.2 MPa after doping with Mg and Zn. Furthermore, Mg additive reduced the solubility of TCP in vitro. Osteoblast culture studies indicated that the presence of Mg stabilized the cell-material interface and thus improved cell attachment and growth. Zn-doped TCP exhibited good bioactivity, which enhanced cell differentiation and alkaline phosphatase (ALP) expression. The highest cell proliferation and ALP expression were found on dual Mg and Zn doped TCP. The results indicate that Mg and Zn dopants play a significant role towards improving mechanical properties and cell-materials interactions of TCP. This work also demonstrates the potential for dual Mg and Zn doped TCP to be used in orthopedics and dentistry, which displays high mechanical strength, low resorption and improved cell-material interaction.

W. Xue · K. Dahlquist · A. Banerjee · A. Bandyopadhyay · S. Bose (✉)
W. M. Keck Biomedical Materials Research Laboratory, School of Mechanical and Materials Engineering, Washington State University, Pullman, WA, USA
e-mail: sbose@wsu.edu

W. Xue
e-mail: weichang_xue@wsu.edu

1 Introduction

Zinc (Zn) is an essential trace element with stimulatory effects on bone formation. In vitro studies showed that Zn has direct specific proliferative effect on osteoblastic cell [1] and a potent and selective inhibitory effect on osteoclastic bone resorption [2, 3]. In vivo study on Zn doped calcium phosphates on rabbit femora showed over 50% more newly formed bone over Zn-free calcium phosphate composition [4]. Recent study also showed relationship between osteoporosis and Zn deficiency in elderly subjects [5].

Recently, Zn-doped calcium phosphate ceramics have also been developed as Zn carrier because of their good biocompatibility. It has been reported that Zn can be incorporated into hydroxyapatite (HA) by substitution of Ca [6–8]. However, the release of Zn from Zn-doped HA is very slow due to low solubility of HA. Zn-doped tricalcium phosphate (TCP) has also been studied in past several years [9–13]. Zn-doped TCP exhibits stimulatory effects on osteoblast bioactivity and bone formation, but also have some drawbacks. As a resorbable ceramic, TCP shows high solubility in vitro or in vivo. Rapid dissolution of TCP results in Zn ion release at high level, which may cause severe toxicity reactions [4, 14]. In addition, TCP ceramic is difficult to be sintered well due to phase transformation from β to α-TCP when sintering at high temperature, which degrades its mechanical properties.

Mg is also one of the most important bivalent ions, which is an important factor in the qualitative changes in the bone matrix that determines bone fragility. Mg

depletion adversely affects all stages of skeletal metabolism, causing low bone growth, decreases osteoblastic and osteoclastic activities [15]. It has been reported that Mg can be incorporated into TCP structure by substitution of Ca [16–19]. Mg improves thermal stability of TCP which prevents phase transformation at high temperature. Furthermore, addition of Mg reduces the resorption of TCP. It has been reported that the solubility of Mg containing TCP decrease with increasing Mg content [20, 21].

In this study, a new approach has been developed to prepare TCP ceramic using dual dopants of Mg and Zn, which combines both benefits of Mg and Zn additives. The presence of Mg enables TCP to be sintered at higher temperature without phase transformation, and thus obtains better mechanical properties and low solubility, while Zn additive also endows TCP with good cell-material interactions. Dual Mg and Zn doped TCP ceramic was synthesized via wet precipitation process. Phase composition and microstructures of ceramics were characterized, and mechanical properties and dissolution behavior were investigated in vitro. Biocompatibility was also evaluated in vitro using human osteoblast cells.

2 Materials and methods

2.1 Sample preparation and characterization

Based on preliminary data of our study using commercial TCP [22], four compositions were synthesized in this study: TCP, TCP doped with 1 wt% MgO (TCP–Mg), TCP doped with 0.3 wt% ZnO (TCP–Zn) and TCP doped with the combination of 1 wt% MgO and 0.3 wt% ZnO (TCP–Mg–Zn). For Mg and Zn doped TCP samples, (Ca+Mg)/P, (Ca+Zn)/P and (Ca+Mg+Zn)/P molar ratio are kept at 1.5. TCP powder was synthesized by a wet coprecipitation method. 1 M Ca^{2+} aqueous solution was made by dissolving 0.1 moles of calcium nitrate ($Ca(NO_3)_2 \cdot 4H_2O$, J. T. Baker, NJ) in 100 ml distilled water. 0.0667 moles of phosphoric acid (H_3PO_4, Fisher Scientific, NJ) was added to that aqueous solution to maintain Ca^{2+} to PO_4^{3-} ratio 1.5 to 1, similar to TCP. The pH of the precursor solution was between 2 and 3. Dropwise addition of ammonium hydroxide (NH_4OH, J. T. Baker, NJ) gradually increased pH of the solution, when precipitation appeared. Final pH of the solution was maintained at 7. Resulting precipitate was filtered and dried at 120°C for 12 h. After drying, precipitate was grinded into a powder and placed in the furnace for calcinations at 650°C for 2 h. TCP–Mg, TCP–Zn and TCP–Mg–Zn powders were also prepared by adding required amount of magnesium nitrate ($Mg(NO_3)_2 \cdot 6H_2O$, J. T. Baker, NJ) and zinc nitrate ($Zn(NO_3)_2 \cdot 6H_2O$, J. T. Baker, NJ) in the solution, and the same precipitation process was followed.

The powders obtained were pressed by uniaxial pressing with a pressure of 10 MPa, and sintered at 1,100 and 1,250°C for 2 h, respectively. The surface morphologies and microstructures of sintered samples were observed using a scanning electron microscope (SEM, Hitachi s-570, Japan). Phase analyses were performed by an X-ray diffractometer (Philips PW 3040/00 X'pert MPD). The relative density was determined by the Archimedian's method. The compressive strength was measured using a mechanical test machine (Instron) with a loading rate of 0.5 mm/min.

2.2 Dissolution in vitro

All samples were immersed in Tris–HCl buffer solution to observe their dissolution behavior. The Tris–HCl buffer solution was prepared by dissolving 50 mM Tris–hydroxymethyl-aminomethane ($(CH_2OH)_3CNH_2$) in distilled water. It was then buffered at pH 7.40 and pH 5.0 with hydrochloric acid (HCl) at 37°C. The masses of the samples were measured after immersion for 7, 14, 21 and 28 days, respectively. The surface morphologies of samples after immersion were observed under SEM.

2.3 Cell culture

All samples were sterilized by autoclaving at 121°C for 20 min. In this study the cells used were an immortalized, cloned osteoblastic precursor cell line 1 (OPC1), which was derived from human fetal bone tissue [23]. OPC1 cells were seeded onto the samples placed in 24-well plates. Initial cell density was 2.0×10^4 cells/well. 1 ml of McCoy's 5A medium (enriched with 5% fetal bovine serum, 5% bovine calf serum and supplemented with 4 μg/ml of fungizone) was added to each well. Cultures were maintained at 37°C under an atmosphere of 5% CO_2. Medium was changed every 2–3 days for the duration of the experiment. Samples for testing were removed from culture at 4, 10 and 28 days of incubation.

2.4 MTT assay

The MTT assay (Sigma, St. Louis, MO) was performed to assess cell proliferation. The MTT solution of 5 mg/ml was prepared by dissolving MTT in PBS, and filter sterilized. The MTT was diluted (50 μl into 450 μl) in serum free, phenol red-free Dulbeco's minimum essential medium (DME). 500 μl diluted MTT solution was then added to each sample in 24-well plates. After 2 h incubation, 500 μl of solubilization solution made up of 10% Triton X-100, 0.1 N HCl and isopropanol were added to dissolve the formazan crystals.

100 µl of the resulting supernatant was transferred into a 96-well plate, and read by a plate reader at 570 nm.

2.5 Morphology of OPC1 cells on samples

All samples for SEM observation were fixed with 2% paraformaldehyde/2% glutaraldehyde in 0.1 M cacodylate buffer overnight at 4°C. Post-fixation was performed with 2% osmium tetroxide (OsO_4) for 2 h at room temperature. The fixed samples were then dehydrated in an ethanol series (30%, 50%, 70%, 95% and 100% three times), followed by a hexamethyldisilane (HMDS) drying procedure. After gold coating, the samples were observed under SEM.

2.6 Immunocytochemistry and confocal microscopy

Samples bearing cells were fixed in 4% paraformaldehyde in 0.1 M phosphate buffer. Those samples were stored at 4°C, for future use. After rinsing in Triton X-100 for 10 min, samples were blocked with TBST/BSA (tris-buffered saline with 1% bovine serum albumin, 250 mM NaCl, pH 8.3) for 1 h. Primary antibody against alkaline phosphatase (ALP) was added at a 1:100 dilution and incubated at room temperature for 2 h. The secondary antibody, goat anti-mouse (GAM) Oregon green (Molecular Probes, Eugene, OR), was added at a 1:100 dilution and incubated for 1 h. Samples were then mounted on coverslips with Vectashield® Mounting Medium (Vector Labs, Burlingame, CA) with propidium iodide (PI) and observed using a confocal scanning laser microscopy (BioRad 1024 RMC).

2.7 Statistical method

Data for relative density, compressive strength and MTT test are presented as mean±standard deviation. Statistical analysis was performed using Student's *t*-test, and $P < 0.05$ was considered statistically significant.

3 Results

3.1 Samples characterization

Figure 1 shows the influence of Mg and Zn additions on densification of TCP ceramics. After sintering at 1,100°C, pure TCP showed low relative density, 74.7% of theoretical density (TD). Addition of Mg did not change the densification of TCP ceramics. However, addition of Zn increased density up to 83.9% of TD for TCP–Zn and 81.5% of TD for TCP–Mg–Zn. After sintering at 1,250°C, the relative density of pure TCP had a small increase compared to 1,100°C sintered samples. TCP–Mg showed a significant increase of density up to 92.9% of TD. A maximum of 99.3% of TD was achieved for TCP–Mg–Zn at 1,250°C.

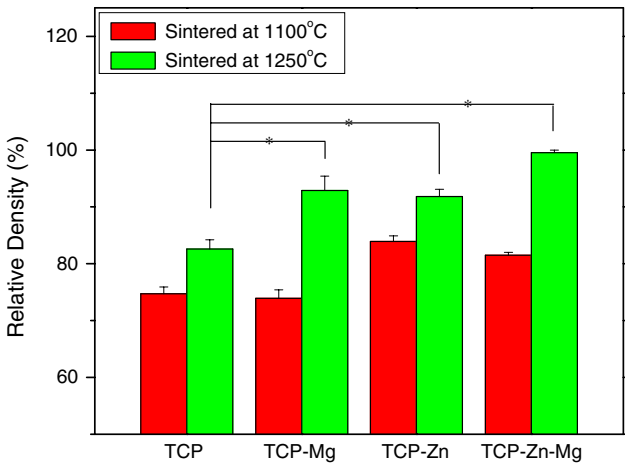

Fig. 1 Relative density of pure and doped TCP samples sintered at 1,100 and 1,250°C (*$P < 0.05$, $n = 5$)

XRD analyses of all samples are shown in Fig. 2. After sintering at 1,100°C, pure β-TCP phase was obtained for all four samples. When sintering temperature increased up to 1,250°C, α-TCP peaks were observed in TCP and TCP–Zn, indicating phase transformation occurred from β to α-TCP. However, all peaks in the patterns of TCP–Mg and TCP–Mg–Zn were from β-TCP, in which no α-TCP peak could be detected. In addition, small shift in peak positions was observed in TCP–Mg and TCP–Mg–Zn.

Figure 3 shows SEM morphologies of the surface of the samples sintered at 1,250°C. On pure TCP, large amount of porosity in the microstructure were observed. Addition of Zn increased densification due to glassy phase formation as observed in Fig. 3c. This glassy phase covered the surface of the grains and therefore no clear grain boundary was observed in the sintered structure. Addition of Mg increased the density of sintered TCP sample as shown in Fig. 3b. TCP–Mg–Zn was sintered well and an almost fully dense microstructure was obtained (Fig. 3d).

Compressive strengths of all samples sintered at 1,250°C are presented in Fig. 4. Pure TCP showed low strength of 24.0 MPa. Addition of Zn and Mg improved compressive strength to 37.8 and 40.4 MPa, respectively. Highest compressive strength of 77.2 MPa was obtained for TCP–Mg–Zn.

3.2 Dissolution behaviour

The dissolution behaviour of all samples was evaluated in Tris-buffer solution, and the results were shown in Fig. 5. Pure TCP showed high dissolution rate. With the addition

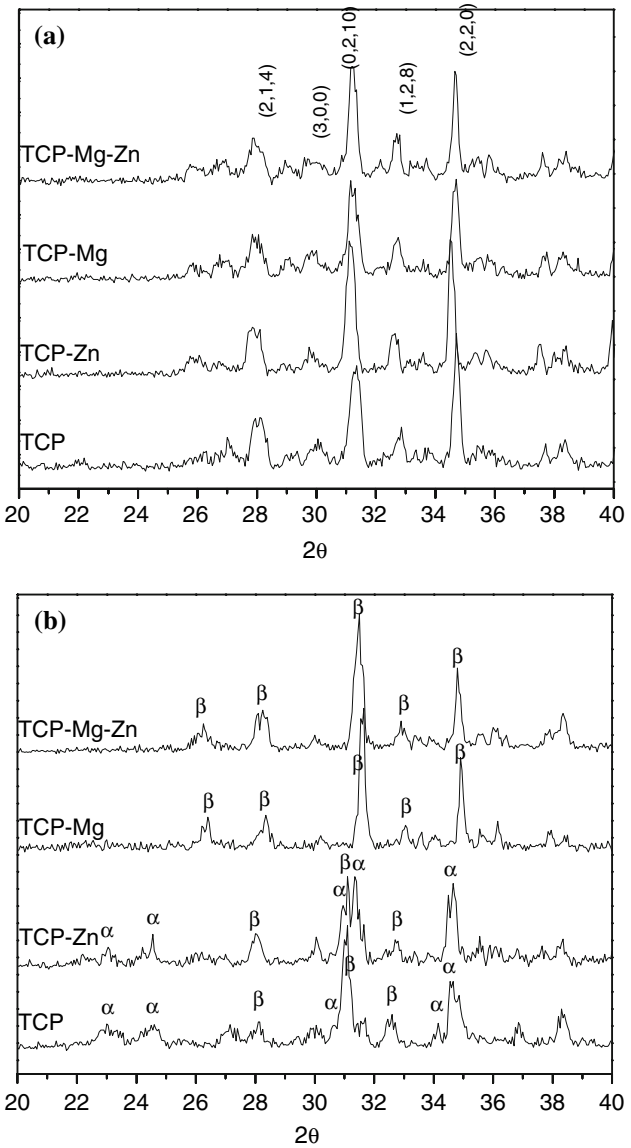

Fig. 2 XRD patterns of samples sintered at: (**a**) 1,100°C, all peaks are attributed to β-TCP; (**b**) 1,250°C, α-TCP peaks are observed in TCP and TCP–Zn

of Mg, the solubility of TCP–Mg and TCP–Mg–Zn decreased significantly. TCP–Zn showed a small decrease of solubility compared with pure TCP, but it still at higher level when compared to Mg-doped samples.

3.3 Cell culture

The MTT assay was used to determine OPC1 cell proliferation on the samples. Figure 6 shows a comparison of cell densities on all samples over the course of experiment. Pure TCP showed low cell density at all time points. The numbers of the cells on TCP–Mg and TCP–Zn were significantly higher than those on pure TCP. A maximum cell density was obtained with TCP–Mg–Zn.

Figure 7 shows SEM morphologies of OPC1 cells on samples after 4 days of culture. Fewer cells distributed on pure TCP. Cells exhibited elongated, flattened morphology with few filopodia extensions, which indicate that cells fail to attach and spread well on TCP surface. Cells on TCP–Mg and TCP–Zn appeared cuboidal and three-dimensional morphology, with some filopodia extensions. More cells distribution was found on the surface of TCP–Mg–Zn. Cells appeared with numerous lamellipodia and filopodia extensions, indicating excellent cell attachment and spreading.

After 28 days of culture, cells on all samples became elongated and confluent together (Fig. 8). More cells were observed on TCP–Mg–Zn, which form a dense and confluent cellular multilayer. The cells synthesized an abundant amount of extracellular matrix (ECM), forming a three-dimensional fibril network (Fig. 8b). Numerous apatite-like granules were precipitated on the surface of cells, revealing the start of mineralization of ECM.

Figure 9 shows confocal micrographs of ALP expression in OPC1 cells cultured on different samples. After 10 days of culture, no ALP product could be observed on pure TCP. The cells on TCP–Mg also showed low ALP expression where only a small signal could be detected. However, cells on TCP–Zn and TCP–Mg–Zn exhibited strong ALP expression. After 28 days of culture, high ALP expressions were obtained on all samples.

4 Discussion

XRD analysis shows no new phase in TCP after doped with Mg and Zn. This result indicates that Mg and Zn are incorporated into the crystal structure of TCP in place of Ca. Because of smaller ionic radius, Mg and Zn reside closer to the axis of cluster than Ca atom [24]. The changes in crystal structure due to the substitution of Mg and Zn also can be demonstrated by XRD analysis in Fig. 2b, showing slight shift in peak position for TCP–Mg and TCP–Mg–Zn. This result is consistent with previous reports [18, 25]. When Mg and Zn are substituted into the TCP structure, Mg–O and Zn–O bonds are stronger than Ca–O bonds due to their short bond length compared to the Ca–O interaction [24]. Therefore, Mg and Zn dopants help to stabilize the structure of TCP and thus improve their mechanical properties.

According to phase diagram [26], β-TCP is stable up to 1,125°C, and between 1,125°C and 1,430°C, α-TCP becomes the stable phase. Presence of α-TCP phase in β-TCP is unwanted due to higher dissolution rate of the former which degrades the strength of TCP ceramics [27,

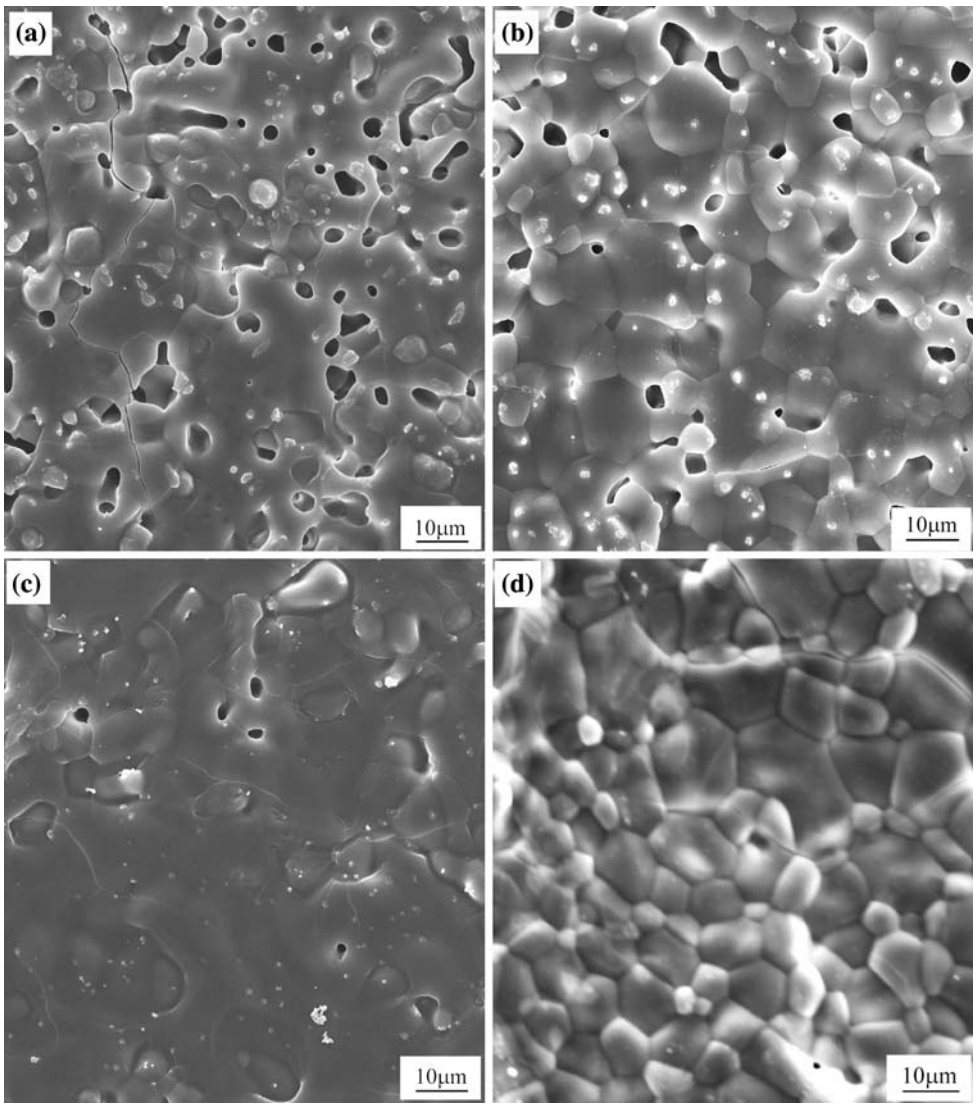

Fig. 3 SEM surface morphologies of the samples sintered at 1,250°C: (**a**) Pure TCP; (**b**) TCP–Mg; (**c**) TCP–Zn; and (**d**) TCP–Mg–Zn

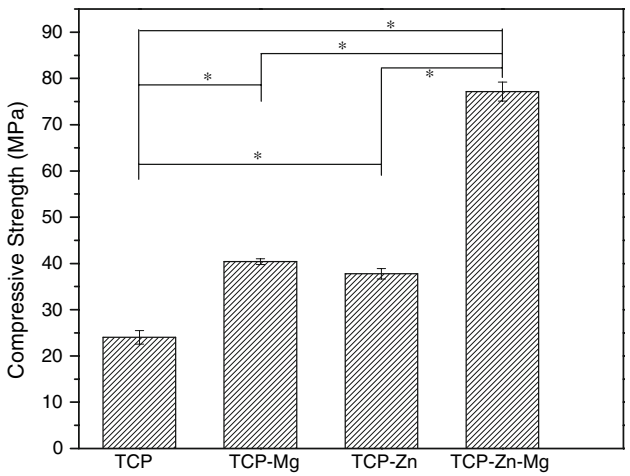

Fig. 4 Compressive strength of the samples sintered at 1,250°C (*$P < 0.05$, $n = 5$)

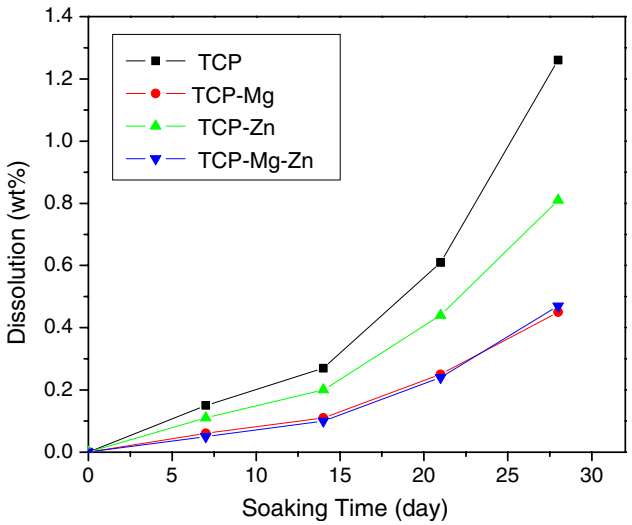

Fig. 5 Dissolution behaviour of the samples sintered at 1,250°C after immersion in Tris–HCl buffer solution at pH 7.4

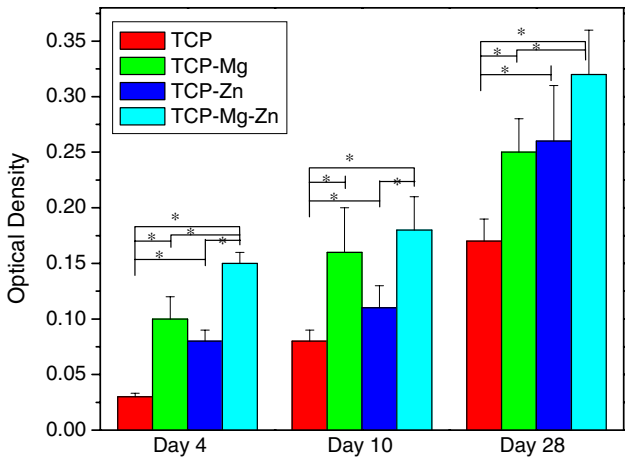

Fig. 6 OPC1 cells proliferation on pure and doped TCP samples ($*P < 0.05$, $n = 4$)

28]. Pure β-TCP ceramic has low sinter density and poor mechanical properties, because of lower sintering temperature to avoid the β to α-TCP phase transformation. In this study, pure TCP shows low relative density after sintering at 1,100°C. Sintering at higher temperature (1,250°C) improves the densification, but phase transformation from β to α-TCP took place as shown in Fig. 2. Phase transformation not only leads to the formation of more soluble α-TCP phase, but also prevents further densification due to the volume expansion during phase transformation [29, 30].

Zn dopant has been demonstrated to restrain phase transformation [31], but it works only when higher content of Zn was used. However, some concerns are raised regarding cytotoxicity of Zn doped compositions higher than 0.316 wt% [4]. Therefore, in this study, 0.3 wt% Zn have been considered. The results indicate that it does not prevent the phase transformation from β to α-TCP. α-TCP also can be found in TCP–Zn composition after sintering at 1,250°C. As a sintering additive, Mg is found to stabilize the β-TCP phase at higher temperature, and increase the phase transformation temperature. Addition of 1 wt% Mg in TCP prevents β to α-TCP phase transformation. Pure β-TCP phase is obtained in TCP–Mg and TCP–Mg–Zn compositions sintered at 1,250°C. The improvement in thermal stability of Mg-doped TCP enables it to be sintered at higher temperature without phase transformation. TCP–Mg–Zn shows the highest sinter density, and thus better mechanical properties.

To understand the influence of dopants on the dissolution rate of TCP, compacts are immersed in Tris–HCl buffer solution. The results indicate that pure TCP has high dissolution rate, which can be attributed towards the presence of α-TCP that is more soluble than β-TCP. In addition, high porosity and low mechanical strength are also important reasons for fast dissolution of pure TCP. The addition of Zn has demonstrated to decrease the solubility of TCP. It is reported that the solubility of Zn doped TCP decreases with increasing zinc content [12]. In this study, the dissolution rate of TCP–Zn shows a small decrease compared to pure TCP, but it is still at a higher level when compared to TCP–Mg and TCP–Mg–Zn. Low content of Zn (0.3 wt%) used and the presence of α-TCP

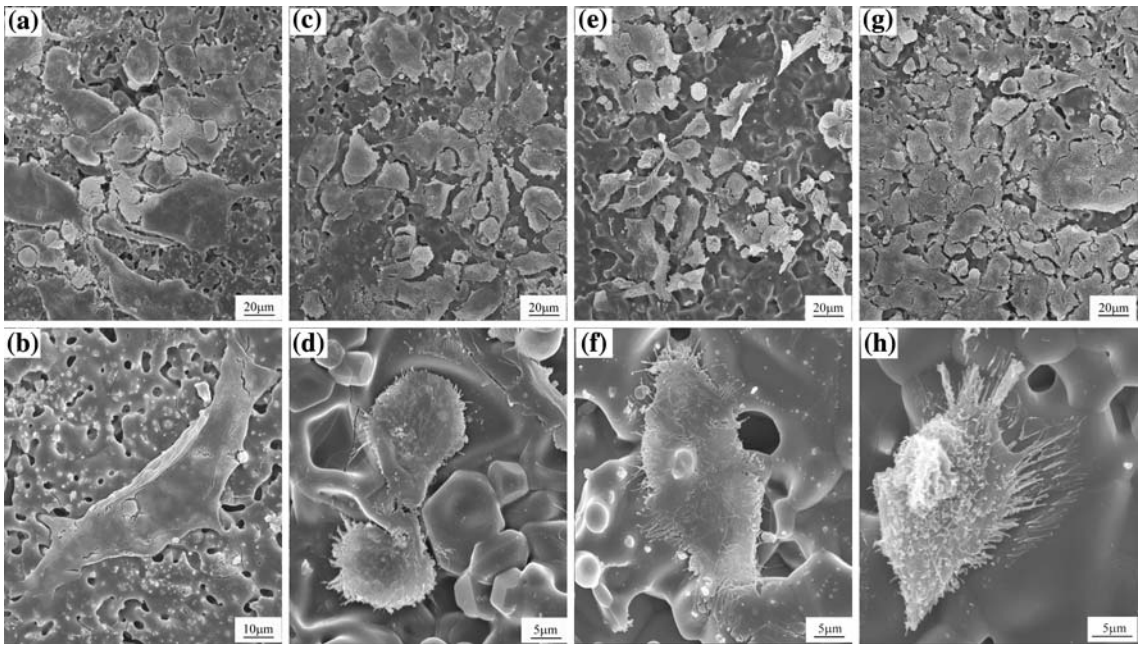

Fig. 7 SEM morphologies of OPC1 cells on samples after 4 days of culture: (**a**, **b**) TCP, (**c**, **d**) TCP–Mg, (**e**, **f**) TCP–Zn and (**g**, **h**) TCP–Mg–Zn

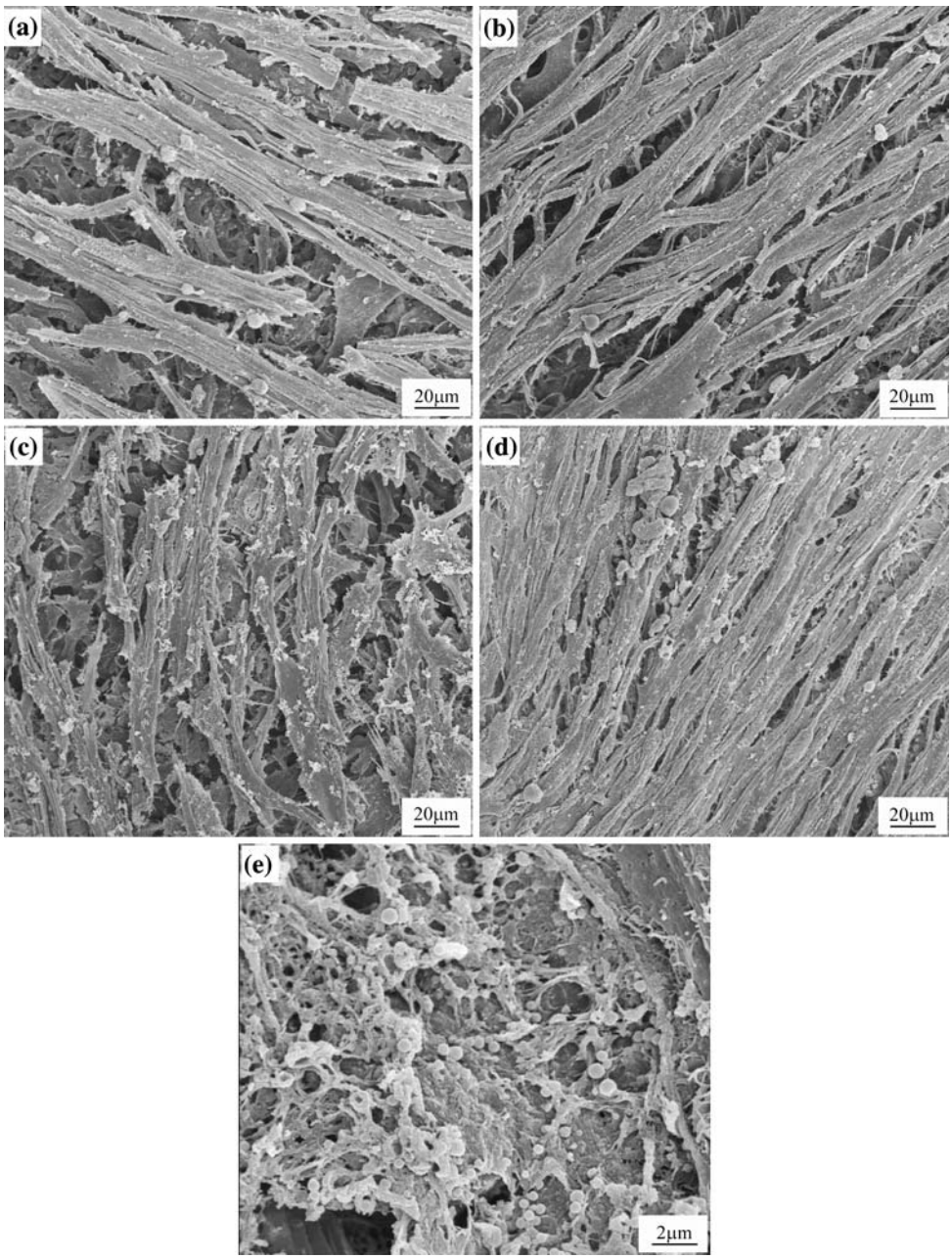

Fig. 8 SEM morphologies of OPC1 cells on samples after 28 days of culture: (**a**) TCP; (**b**) TCP–Mg; (**c**) TCP–Zn; and (**d**, **e**) TCP–Mg–Zn

are the reasons for high solubility of TCP–Zn. However, Mg is found to reduce the resorption of TCP significantly. Both TCP–Mg and TCP–Mg–Zn display lower dissolution rate in vitro compared to undoped TCP. The decrease in resorption of Mg-doped TCP helps to control the release of Zn and provide a stable cell-material interface.

A stable cell-material interface is crucial to support cell adhesion and subsequent proliferation and differentiation. The establishment of cell-material interface mainly depends on material surface properties, including surface chemistry and topography. With respect to bioresorbable TCP ceramics, the dissolution behavior plays a critical role in the cell response. In this study, undoped TCP shows high solubility, which damages the stability of cell-material interface. Therefore, cells fail to attach well and spread on material surface. The dissolution of TCP at cell-material interface affects cell proliferation and differentiation, which explains why low cell density and ALP expression are seen with this material.

It has been demonstrated that Zn promotes the activity of osteoblast and stimulated bone formation [1]. In our study, high ALP expression on TCP–Zn indicates this material enhances cell differentiation. However, high solubility of TCP–Zn influences cell proliferation, which results in lower cell density compared with TCP–Mg–Zn. The addition of Mg reduces the solubility of TCP–Mg,

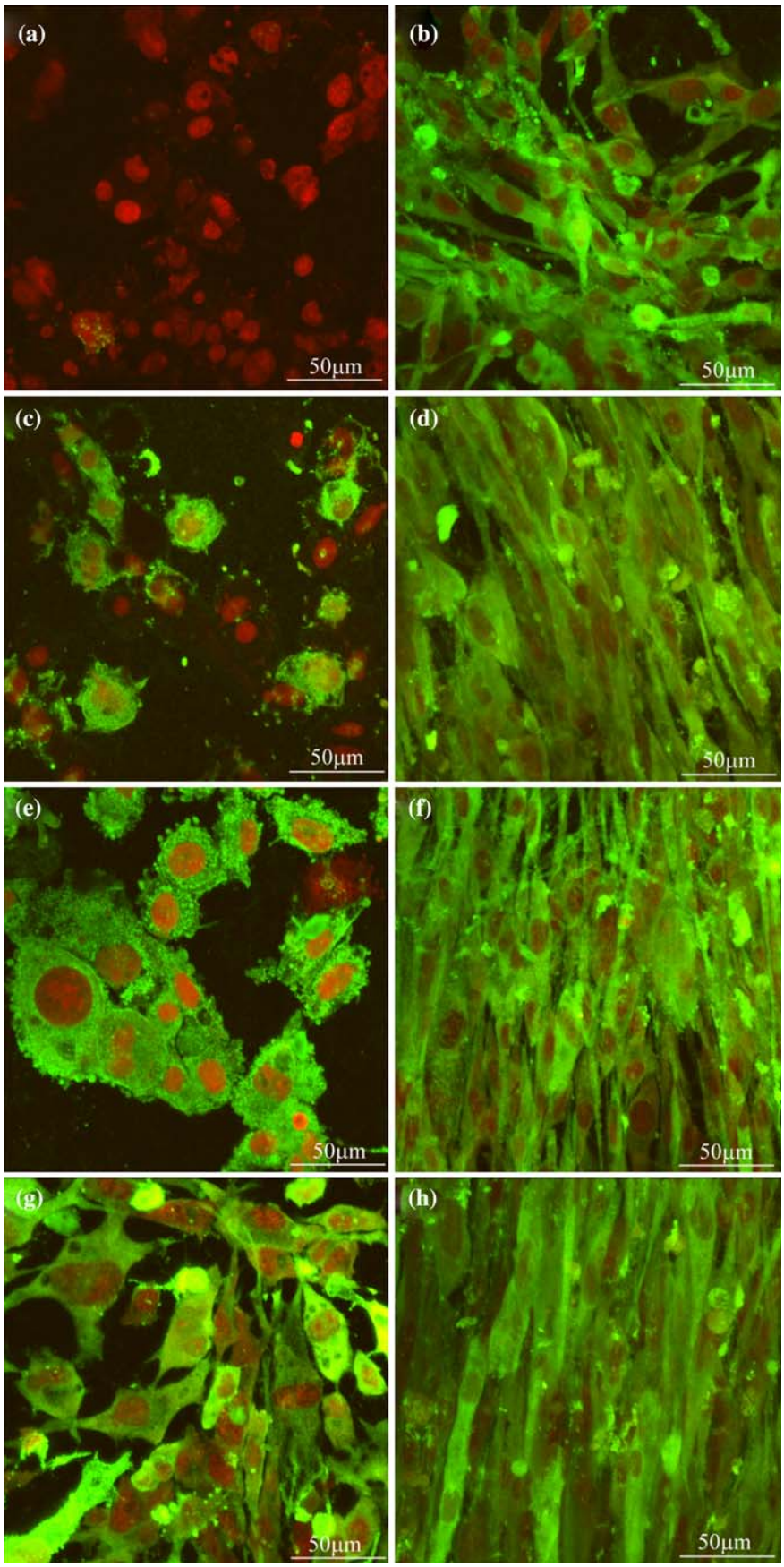

Fig. 9 Confocal micrographs of ALP expression in OPC1 cells cultured on (**a**) TCP at day 10, (**b**) TCP at day 28, (**c**) TCP–Mg at day 10, (**d**) TCP–Mg at day 28, (**e**) TCP–Zn at day 10, (**f**) TCP–Zn at day 28, (**g**) TCP–Mg–Zn at day 10 and (**h**) TCP–Mg–Zn at day 28. Green fluorescence indicates antibody bound to ALP, red fluorescence indicates nucleus

which is helpful to establish stable cell-material interface, thus enhances cell attachment and proliferation. Thus, higher cell attachment and growth are obtained on TCP–Mg and TCP–Mg–Zn sample surfaces, when compared with undoped TCP. With dual dopants of Mg and Zn, TCP–Mg–Zn shows highest cell proliferation, which can be attributed to Mg additive. Furthermore, the presence of Zn also helps to stimulate cell differentiation, showing the highest ALP expression on this material.

5 Conclusions

TCP ceramics with dual dopants of Mg and Zn were synthesized by precipitation process. The addition of Mg improved thermal stability and prevented phase transformation from β to α-TCP, which increased compression strength of dense materials from 24.0 MPa to 77.2 MPa after doping with Mg and Zn. The presence of Mg also reduced solubility, which stabilized cell-material interface and thus improved cell attachment and growth. Zn-doped TCP exhibited good bioactivity with stimulating cell differentiation and ALP expression, but had high solubility. TCP with dual dopants combined the benefits of Mg and Zn additives. The presence of Mg enabled TCP–Mg–Zn to obtain high mechanical property, low solubility and good cell-material interaction while Zn additive stimulated osteoblast response. The results obtained indicate that TCP with dual dopants of Mg and Zn has the potential to be used in orthopedics and dentistry.

Acknowledgements The authors gratefully acknowledge the financial support from National Science Foundation (Grant # 0134476) and the Office of Naval Research (Grant Nos: N00014-1-04-0644 and N00014-1-05-0583).

References

1. M. Hashizume, M. Yamaguchi, Mol. Cell. Biochem. **122**, 59 (1993)
2. S. Kishi, M. Yamaguchi, Biochem. Pharmacol. **48**, 1225 (1994)
3. B.S. Moonga, D.W. Dempster, J. Bone Miner. Res. **10**, 453 (1995)
4. H. Kawamura, A. Ito, S. Miyakawa, P. Layrolle, K. Ojima, H. Naito, N. Ichnose, T. Tateishi, J. Biomed. Mater. Res. **50**, 184 (2000)
5. T.H. Hyun, E. Barrett-Connor, D.B. Milne, Am. J. Clin. Nutr. **80**, 715 (2004)
6. E. Fujii, M. Ohkubo, K. Tsuru, S. Hayakawa, A. Osaka, K. Kawabata, C. Bonhomme, F. Babonneau, Acta Biomaterialia. **2**, 69 (2006)
7. H. Storrie, S.I. Stupp, Biomaterials **26**, 5492 (2005)
8. Y. Sogo, A. Ito, K. Fukasawa, T. Sakurai, N. Ichinose, Mater. Sci. Tech. **20**, 1079 (2004)
9. A. Ito, M. Otsuka, H. Kawamura, M. Ikeuchi, H. Ohgushi, Y. Sogo, N. Ichinose, Curr. Appl. Phys. **5**, 402 (2005)
10. M. Otsuka, Y. Ohshita, S. Marunaka, Y. Matsuda, A. Ito, N. Ichinose, K. Otsuka, W.I. Higuchi, J. Biomed. Mater. Res. Part A **69**, 552 (2004)
11. H. Kawamura, A. Ito, T. Muramatsu, S. Miyakawa, N. Ochiai, T. Tateishi, J. Biomed. Mater. Res. Part A **65**, 468 (2003)
12. A. Ito, H. Kawamura, S. Miyakawa, P. Layrolle, N. Kanzaki, G. Treboux, K. Onuma, S.T. Sutsumi, J. Biomed. Mater. Res. **60**, 224 (2002)
13. A. Tas, S.B. Bhaduri, S. Jalota, Mater. Sci. Eng. C **27**, 394 (2007)
14. A. Bandyopadhyay, E.A. Withey, J. Moore, S. Bose, Mater. Sci. Eng. C **27**, 14 (2007)
15. M. Percival, Appl. Nutr. Sci. Rep. **5**, 1 (1999)
16. K. Yoshida, N. Kondo, H. Kita, J. Am. Ceram. Soc. **88**, 2315 (2005)
17. B. Dickens, L.W. Schroeder, W.E. Brown, J. Sol. Stat. Chem. **10**, 232 (1974)
18. L.W. Schroeder, B. Dickens, W.E. Brown, J. Sol. Stat. Chem. **22**, 253 (1977)
19. R. Enderle, F. Gotz-Neunhoeffer, M. Gobbels, F.A. Muller, P. Greil, Biomaterials **26**, 3379 (2005)
20. F.H. Lin, C.H. Liao, K.S. Chen, J.S. Sun, C.P. Lin, Biomaterials **22**, 2981 (2001)
21. C. Tardei, F. Grigore, I. Pasuk, S. Stoleriu, J. Optoelectr. Adv. Mater. **8**, 568 (2006)
22. A. Bandyopadhyay, S. Bernard, W.C. Xue, S. Bose, J. Am. Ceram. Soc. **89**, 2675 (2006)
23. S.R. Winn, G. Randolph, H. Uludag, S.C. Wonng, G.A. Hair, J.O. Hollinger, J. Bone Mineral. Res. **14**, 1721 (1999)
24. L. Calderin, X. Yin, M.J. Stott, M. Sayer, Biomaterials **23**, 4155 (2002)
25. J. Marchi, A.C.S. Dantas, P. Greil, J.C. Bressiani, A.H.A. Bressiani, F.A. Muller, Mater. Res. Bull. **42**, 1040 (2007)
26. J.C. Elliot, in *Structure and Chemistry of the Apatites and Other Calcium Orthophosphate*s (Elsvier Science, Amsterdam, 1994)
27. S.R. Radin, P. Ducheyne, J. Biomed. Mater. Res. **27**, 35 (1993)
28. S.R. Radin, P. Ducheyne, J. Biomed. Mater. Res. **28**, 1303 (1994)
29. H.S. Ryu, H.J. Youn, K.S. Hong, B.S. Chang, C.K. Lee, S.S. Chung, Biomaterials **23**, 909 (2002)
30. R. Famery, P.B. Richard, Ceram. Int. **20**, 327 (1994)
31. X. Wei, M. Akinc, in *Advances in Bioceramics and Biocomposites: Ceramic Engineering and Science Proceedings*, vol 26, ed. by D. Zhu, W. Kriven (2005), pp 129